Journal of Hazardous Materials 166 (2009) 547–552

Contents lists available at ScienceDirect

Journal of Hazardous Materials

journal homepage: www.elsevier.com/locate/jhazmat

Visible light photoelectrocatalysis with salicylic acid-modified TiO_2 nanotube array electrode for *p*-nitrophenol degradation

Xin Wang, Huimin Zhao*, Xie Quan, Yazhi Zhao, Shuo Chen

School of Environmental and Biological Science and Technology, Dalian University of Technology, Dalian 116024, China

ARTICLE INFO

Article history:
Received 1 September 2008
Received in revised form
18 November 2008
Accepted 18 November 2008
Available online 27 November 2008

Keywords:
TiO_2 nanotube
Salicylic acid
Photoelectrocatalysis
Nitrophenol
Modification

ABSTRACT

This research focused on immersion method synthesis of visible light active salicylic acid (SA)-modified TiO_2 nanotube array electrode and its photoelectrocatalytic (PEC) activity. The SA-modified TiO_2 nanotube array electrode was synthesized by immersing in SA solution with an anodized TiO_2 nanotube array electrode. Scanning electron microscope (SEM), X-ray diffraction (XRD), X-ray photoelectron spectroscopy (XPS), infrared spectroscopy (IR), UV–vis diffuse reflectance spectrum (DRS), and Surface photovoltage (SPV) were used to characterize this electrode. It was found that SA-modified TiO_2 nanotube array electrode absorbed well into visible region and exhibited enhanced visible light PEC activity on the degradation of *p*-nitrophenol (PNP). The degradation efficiencies increased from 63 to 100% under UV light, and 79–100% under visible light ($\lambda > 400$ nm), compared with TiO_2 nanotube array electrode. The enhanced PEC activity of SA-modified TiO_2 nanotube array electrode was attributed to the amount of surface hydroxyl groups introduced by SA-modification and the extension of absorption wavelength range.

1. Introduction

Photocatalytic (PC) oxidation, a new wastewater treatment or water purification technique, has attracted increasing attentions in the field of environmental protection in the past decades [1]. Among various oxide semiconductor photocatalysts, TiO_2 is one of the most promising photocatalysts because of its non-toxicity, chemical stability, relatively low price, and capability of photooxidative destruction of most organic pollutants [2]. However, its wide band gap (3.2 eV) allows it to absorb only the UV light ($\lambda < 388$ nm) which account for merely 4–5% of the solar energy, thereby hampering its wide application. In view of efficient utilization of solar energy, many attempts have been made including sensitization with dyes [3], combination with narrow band gap semiconductors [4], and doping with nonmetal atoms, such as C [5], N [6], or Si [7].

Recently, most attentions have been given to carbon-doped TiO_2 because it leads to visible-light photocatalysis. Many researches have demonstrated that the high visible light PC activity of carbon-doped TiO_2 is attributed to the lowering of the band gap of TiO_2 [8,9]. Nevertheless, among the studies of carbon-doped TiO_2 for degradation of organics under visible light illumination, Nagaveni et al. [10] observed that a larger amount of surface-adsorbed hydroxyl groups was one of the primary factors contributing to the high PC activity, besides the lowering of the band gap of TiO_2. This result implies that doping with large amounts of hydroxyl groups to the surface of TiO_2 will lead to the increase in PC activity, which may be achieved by modification with the compounds containing hydroxyl groups. Li et al. [11] modified TiO_2 nanoparticles with salicylic acid (SA) which contained hydroxyl groups, and found that SA-modified TiO_2 nanoparticles exhibited enhanced PC activity. However, the high PC activity was attributed to the improved surface coverage of pollutants on the TiO_2 nanoparticles but not the function of hydroxyl groups [11], and this study focused mainly on TiO_2 nanoparticles limiting its application for wastewater treatment due to the difficulty in recovery.

The difficulties in separating TiO_2 nanoparticles from aqueous solution and the high rate of photogenerated electron–hole pair recombination have restricted the application of TiO_2 nanoparticles photocatalysts. To solve the problem of separation, the TiO_2 nanoparticles could be immobilized on a solid substrate, whereas it causes other defects. On one hand, the surface area of the immobilized TiO_2 exposed to the solution is lower than that of the suspended TiO_2. On the other hand, poor adhesion of the TiO_2 film on the supporting substrate can suppress electron transfer [12]. Many reports [13,14] indicated that the TiO_2 nanotubes being formed on the Ti substrate by anodization exhibit good properties comparing with the immobilized TiO_2 film. First, the TiO_2 nanotubes allow more effectively absorption of incident photons, because of an increased light penetration depth and better scattering

* Corresponding author. Tel.: +86 411 84706140; fax: +86 411 84706263.
E-mail address: zhaohuim@dlut.edu.cn (H. Zhao).

0304-3894/$ – see front matter © 2008 Elsevier B.V. All rights reserved.
doi:10.1016/j.jhazmat.2008.11.066

with a regular pore structure. Second, the photogenerated electrons can be fast and efficient transferred leading to a much reduced electron–hole recombination. In addition, there is a growing interest in the synthesis of TiO_2 nanotubes by anodization due to the simplicity in preparation and handling and more controllable synthesis than other methods, such as sol–gel, hydrothermal, and template method. Thus, TiO_2 nanotube arrays anodized on Ti sheet were chosen to be modified with the compounds containing hydroxyl groups to resolve the problems of separation and recovery while to improve the PC efficiency. And photoelectrocatalytic (PEC) process has been demonstrated that it can prevent charge carriers from combining by driving the photogenerated electrons to a counter electrode via the external circuit, consequently improving the efficiency of oxidation.

In this paper, we fabricated TiO_2 nanotube arrays by anodization, and focused on immersion method synthesis of SA-modified TiO_2 nanotube array electrode and its PEC activity. The electrode was characterized by scanning electron microscope (SEM), X-ray diffraction (XRD), X-ray photoelectron spectroscopy (XPS), infrared spectroscopy (IR), UV–vis diffuse reflectance spectrum (DRS), and Surface photovoltage (SPV). The PEC activity of this electrode was evaluated by measuring degradation efficiency of *p*-nitrophenol (PNP), which was of environmental concern and listed as priority pollutants by the U.S. Environmental Protection Agency [15]. It is expected that this kind of electrode might improve the PEC activity and enhance the utilization of visible light.

2. Experimental

2.1. Fabrication of SA-modified TiO_2 nanotube array electrode

The titanium (Ti) sheet (purity 99.6%, thickness 0.5 mm, from Tianjin Gerui Co. Ltd.) was first polished with different abrasive paper, rinsed in an ultrasonic bath of anhydrous alcohol and deionized water for 20 min and 5 min in turn, then chemically etched by immersing it in $HF/HNO_3/H_2O$ (1:4:5, v/v/v) mixed solution, and finally rinsed with deionized water. Anodization was carried out in a two-electrode electrochemical cell, with the treated Ti sheet serving as the anode and a platinum (Pt) foil (purity 99.9%) serving as the cathode. TiO_2 nanotube arrays formed in an electrolyte of 0.5% HF + acetic acid mixed in a 7:1 ratio. Anodization was performed at a constant voltage of 20 V for 20 min. The freshly prepared sample was immediately rinsed with deionized water and dried in the atmosphere. Then, the anodized Ti substrate was calcinated in a muffle oven at 500 °C for 2 h with heating and cooling rates of 2 °C/min to convert the amorphous phase to crystalline phase. Surface modification was carried out by immersing the TiO_2 nanotube arrays in a 100 mg/L aqueous solution of SA for 30 min. The modified TiO_2 nanotube arrays were washed with deionized water and heat-treated for 30 min at 100 °C.

2.2. Characterization

The morphology of the SA-modified TiO_2 nanotube arrays was characterized using a SEM (Quanta 200 FEG) with an accelerating voltage of 30 kV. The XRD patterns were recorded on a Shimadzu LabX XRD-6000 diffractometer using Cu Kα radiation. The surface properties and composition of the sample were analyzed by XPS (AMICUS). IR studies were carried out in 500–4000 cm^{-1} frequency range in the transmission mode (Shimadzu IR Prestige). The DRS measurements were carried out on UV-160A and were recorded in the 800–200 nm range. The SPV measurements were carried out on a commercial KP system (KP Technology Ltd., Scotland, UK).

2.3. PEC experiments

The PEC oxidation of PNP was performed in a single photoelectrochemical compartment which was constructed of a rectangular shaped quartz reactor, a SA-modified TiO_2 nanotube array electrode serving as photo-anode, a Pt wire serving as cathode, and a saturated calomel electrode (SCE) serving as the reference electrode. Bias potentials applied on the photo-anode were 0.8 V (vs SCE). A 300 W high-pressure mercury lamp was used as UV light source; the incident intensities to the electrode surface for UV light irradiation were 1.0 mW/cm^2. A 500 W Xe lamp was used as visible light source and a cutoff filter (JB 400, Huayu Institute of Thinfilm Technology, China) was used to filter the light of which wavelength less than 400 nm; the incident intensities to the electrode surface for visible light irradiation was 27 mW/cm^2. The experiments were performed with magnetic stirring, using 0.01 M sodium sulfate as the electrolyte. The initial concentration of the PNP aqueous solution was 5 mg/L.

2.4. Analytical method

The determination of the PNP concentration was performed by HPLC with a Kromasil ODS (5 μm) reversed-phase column at 25 °C. A mixture of methanol and water, 60:40 (v/v), was used as the mobile phase. PNP was detected at a wavelength of 317 nm.

3. Results and discussion

3.1. Morphology of SA-modified TiO_2 nanotube arrays

Fig. 1 showed SEM images of the TiO_2 nanotube arrays and SA-modified TiO_2 nanotube arrays, respectively. It revealed that well-ordered nanotubes with open top end were formed; the average diameter of these nanotubes was c.a. 80 nm. There was no appreciable surface structure change after the process of SA-modification, which indicated that the modification with SA did not destroy the structure of the nanotubes.

3.2. XRD analysis

The XRD patterns of the TiO_2 nanotube arrays and SA-modified TiO_2 nanotube arrays were displayed in Fig. 2. Anatase phase corresponding to $2\theta = 25.4^\circ$ was crystallized after annealing at 500 °C, and no rutile or any other phases were observed both in the patterns of TiO_2 nanotube arrays and the SA-modified TiO_2 nanotube arrays, indicating that there was no atom of SA substitute for titanium atom in the lattice of the oxide.

3.3. XPS analysis

The C 1s XPS spectra of SA-modified TiO_2 nanotube arrays can be fitted by three peaks: carbon presented in phenol, alcohol, or ether groups (peak a, binding energy (BE) = 286.4 eV), carboxylic acid or ester groups (peak b, BE = 289.3 eV), carbonate, occluded CO or π-electrons in aromatic rings (peak c, BE = 290.0 eV), as shown in Fig. 3. The analysis of the C 1s XPS spectra confirmed the presence of SA on TiO_2 nanotube arrays due to the modification.

3.4. IR analysis

IR spectra of the TiO_2 nanotube arrays and SA-modified TiO_2 nanotube arrays were depicted in Fig. 4. For TiO_2 nanotube arrays, a broad band at 3250–3470 cm^{-1} can be attributed to H-bound water. For SA-modified TiO_2 nanotube arrays, the bands in the region of 3300–3500 cm^{-1} and 1460–1530 cm^{-1} can be attributed to the O-H deformation vibration in carboxyl groups. Compared with TiO_2

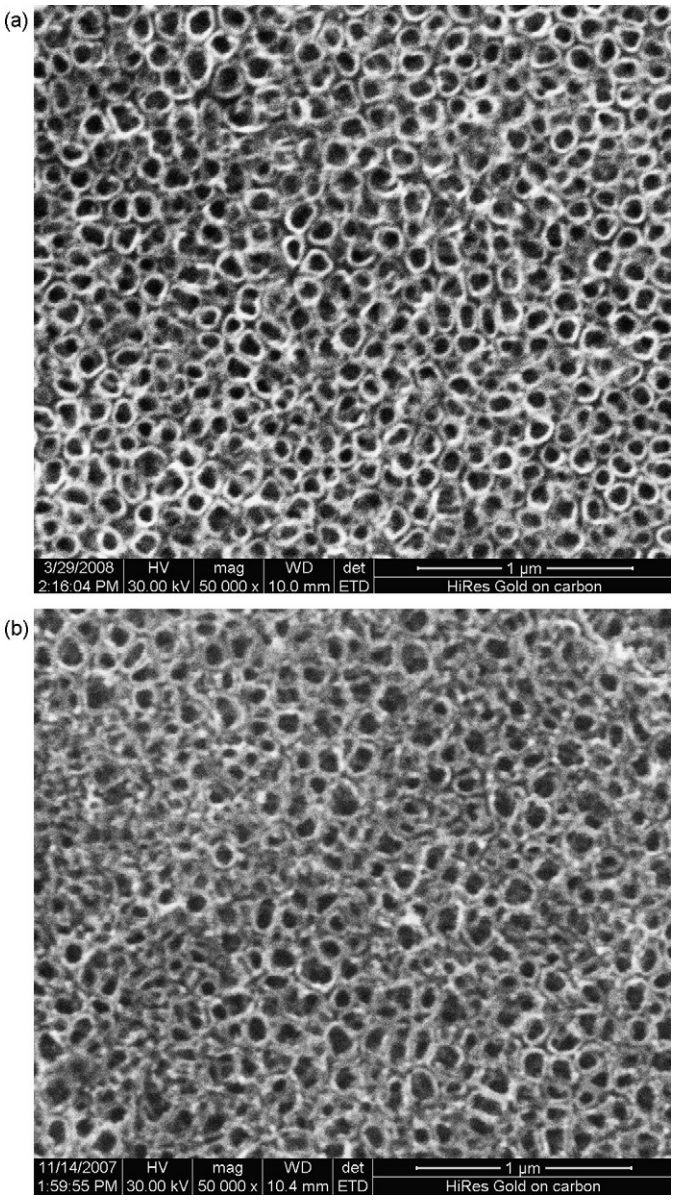

Fig. 1. SEM images of (a) TiO_2 nanotube arrays and (b) SA-modified TiO_2 nanotube arrays.

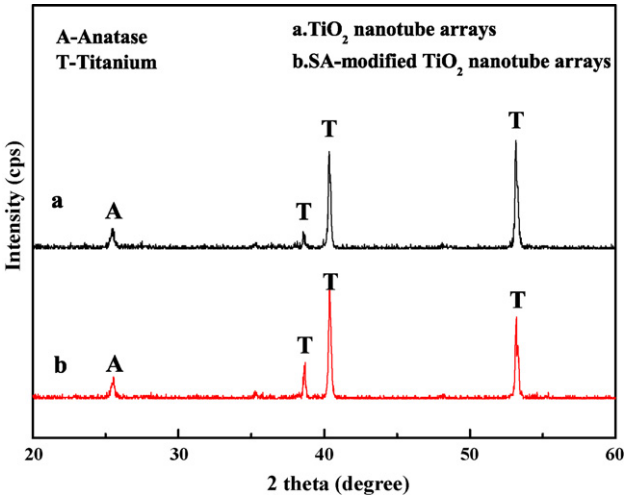

Fig. 2. XRD patterns of TiO_2 nanotube arrays and SA-modified TiO_2 nanotube arrays.

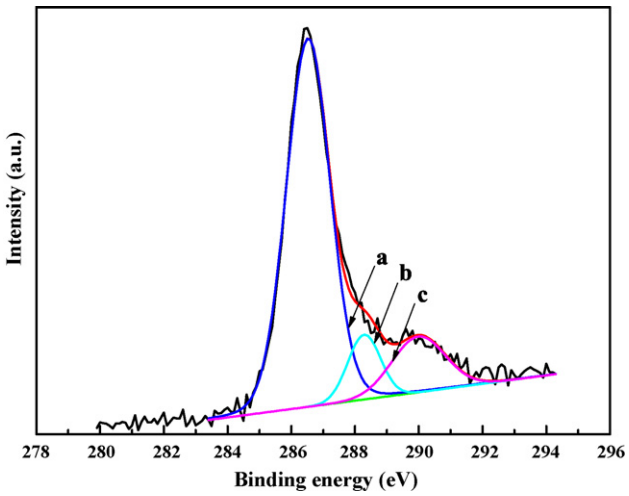

Fig. 3. C 1s XPS spectra of SA-modified TiO_2 nanotube arrays: (a) carbon present in phenol, alcohol, or ether groups; (b) carboxylic acid or ester groups; (c) carbonate, occluded CO or π-electrons in aromatic rings.

nanotube arrays, there was a significant increase of surface hydroxyl groups on the SA-modified TiO_2 nanotube arrays. The bands in the region of 1600–1700 cm^{-1} can be assigned to the C=O stretching vibrations corresponding to carbonyl and carboxyl groups. Through the results of IR, it can be deduced that SA was present on the SA-modified TiO_2 nanotube arrays and provided increased amounts of surface hydroxyl groups.

3.5. DRS analysis

The DRS measurements showed that the modification of SA on TiO_2 nanotube arrays led to a red-shift in the optical response (Fig. 5(a)). Band gap can be determined from the fundamental absorption edge or coefficient. For a indirect band gap material, such as TiO_2, the optical absorption near the band edge follows the equation $(\alpha h\nu)^{0.5} = A(h\nu - E_g)$ [16]. The plots of the $(\alpha h\nu)^{0.5}$ vs $h\nu$ obtained and were shown in Fig. 5(b). The band gap energies of TiO_2 nanotube arrays and SA-modified TiO_2 nanotube arrays were estimated to be 3.33 eV and 3.18 eV, respectively, which revealed that the ability of visible light utilization of SA-modified TiO_2 nanotube arrays would be a little higher than that of TiO_2 nanotube arrays.

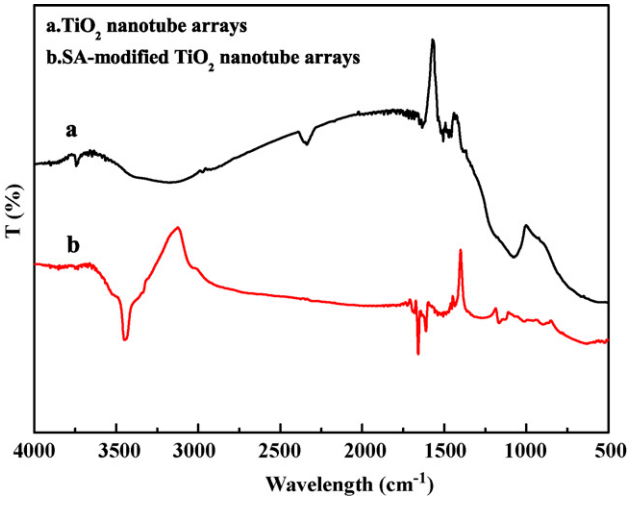

Fig. 4. IR spectra of TiO_2 nanotube arrays and SA-modified TiO_2 nanotube arrays.

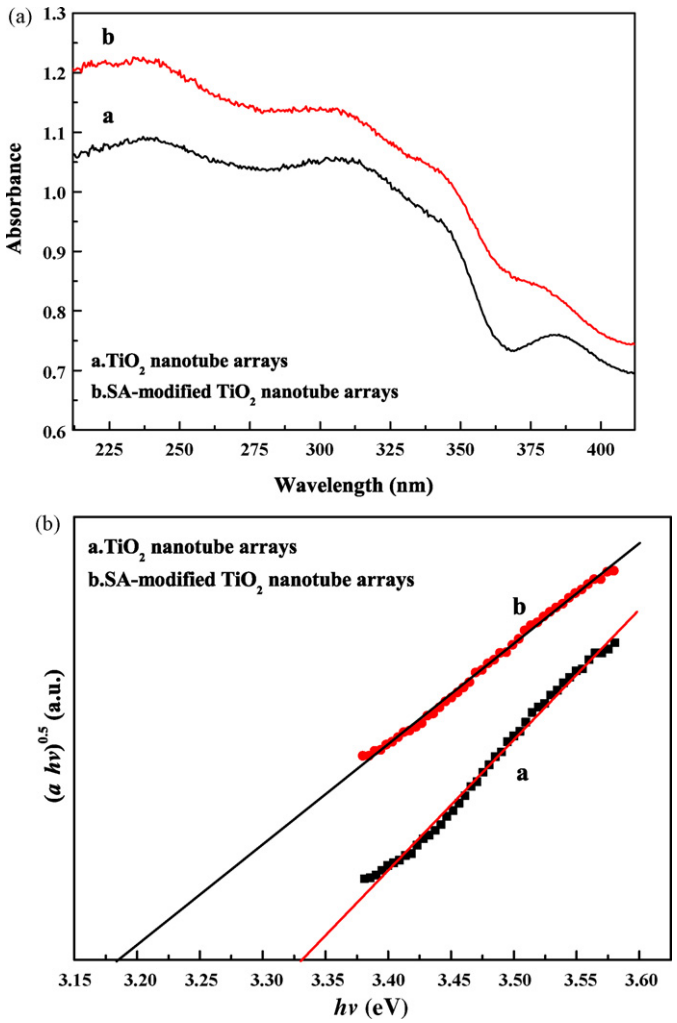

Fig. 5. (a) DRS of TiO_2 nanotube arrays and SA-modified TiO_2 nanotube arrays and (b) fitting curves of $(\alpha h\nu)^{0.5}$ to $h\nu$ of TiO_2 nanotube arrays and SA-modified TiO_2 nanotube arrays.

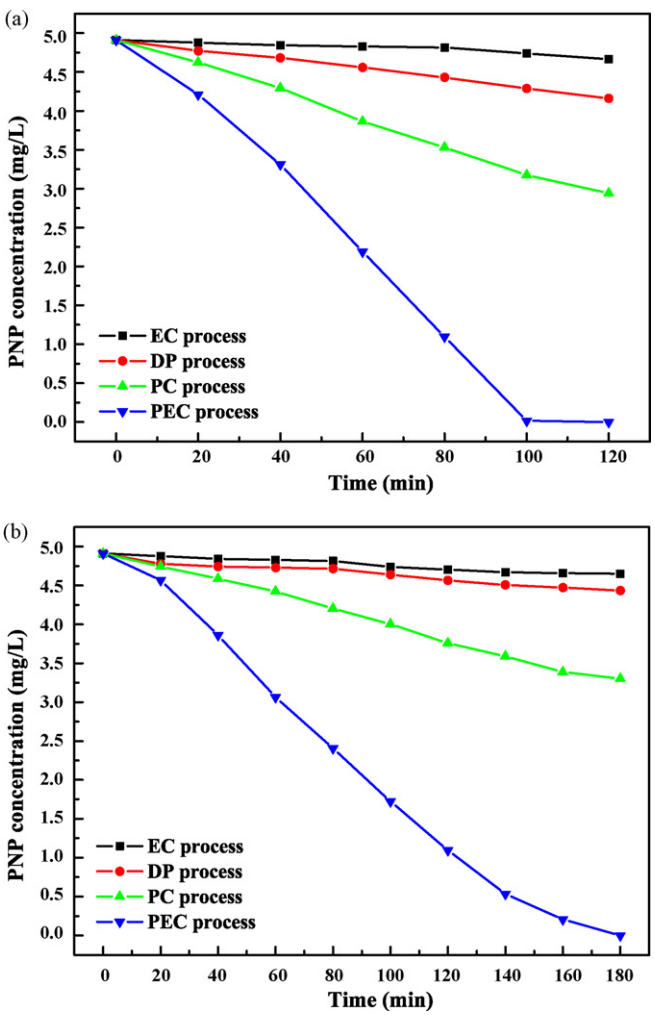

Fig. 7. EC, DP, PC, and PEC degradation of PNP (a) under UV light irradiation (1.0 mW/cm^2, 0.8 V vs SCE) and (b) under visible light ($\lambda > 400$ nm, 27 mW/cm^2, 0.8 V vs SCE) irradiation using SA-modified TiO_2 nanotube array electrode.

3.6. SPV analysis

Fig. 6 displayed the SPV spectra of the TiO_2 nanotube arrays and SA-modified TiO_2 nanotube arrays. A red shift of the excitation band edge was observed and for SA-modified TiO_2 nanotube arrays the surface photovoltage signal was stronger than that of TiO_2 nanotube arrays over the whole tested wavelength range, indicating that a high PC activity could be expected for SA-modified TiO_2 nanotube arrays.

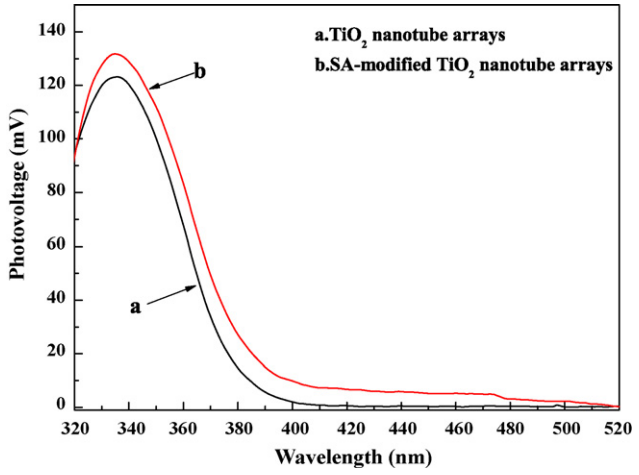

Fig. 6. Surface photovoltage spectra of TiO_2 nanotube arrays and SA-modified TiO_2 nanotube arrays.

3.7. Degradation of PNP

The electrochemical (EC), direct photolytic (DP), PC, and PEC degradation of PNP were performed on the SA-modified TiO_2 nanotube array electrode. Under UV light irradiation, the degradation efficiencies of PNP in 2 h in EC, DP, PC, and PEC processes were 5%, 15%, 40%, and 100%, respectively (Fig. 7(a)), while under visible light irradiation, the degradation efficiencies of PNP in 3 h were 5%, 10%, 33%, and 100%, respectively (Fig. 7(b)). The change of PNP concentration in EC process showed that the bias potential of 0.8 V was not enough to degrade PNP, therefore, it was inferred that the effect of 0.8 V bias potential was mainly to drive the photogenerated electrons away in PEC process. Clearly, the degradation efficiency of PNP in PEC process was larger than the sum of EC and PC process, indicating that a sort of synergetic effect occurred during the PEC process and enhanced the PNP degradation efficiency on SA-modified TiO_2 nanotube array electrode under UV and visible light irradiation.

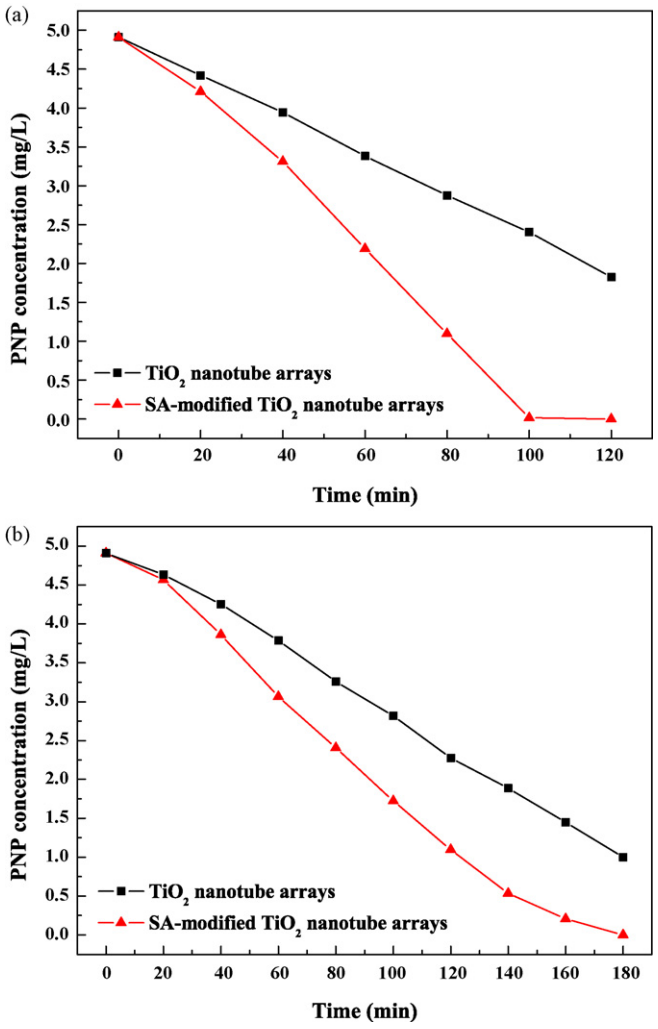

Fig. 8. Variation of PNP concentrations by PEC technology with TiO_2 nanotube array electrode and SA-modified TiO_2 nanotube array electrode (a) under UV light irradiation (1.0 mW/cm^2, 0.8 V vs SCE) and (b) under visible light ($\lambda > 400$ nm, 27 mW/cm^2, 0.8 V vs SCE) irradiation.

3.8. PEC activity

The degradation efficiencies of SA-modified TiO_2 nanotube array electrode were much higher than that of the non-modified one. Under UV light irradiation, in 2 h, 100% of PNP was degraded by SA-modified TiO_2 nanotube array electrode, while only 63% of PNP was degraded by TiO_2 nanotube array electrode (Fig. 8(a)). Meanwhile, under visible light irradiation, in 3 h, 100% of PNP was degraded by SA-modified TiO_2 nanotube array electrode, in contrast, 79% of PNP was degraded by TiO_2 nanotube array electrode (Fig. 8(b)). These results were consistent with that of DRS and SPV, which would be attributed to the improved utilization of visible light and the increased amounts of surface hydroxyl groups which accepted holes generated by solar or UV illumination to form hydroxyl radicals thus preventing electron–hole recombination.

3.9. Stability of SA-modified TiO_2 nanotube array electrode

To test the stability of SA-modified TiO_2 nanotube array electrode, the electrode was reused 10 times. The repeated experiments were performed in 2 h under UV light irradiation under similar conditions mentioned above. PNP was almost decomposed after 2 h irradiation. The results demonstrated that the degradation efficiencies of PNP were rather stable with the RSD of 1.4% (Fig. 9).

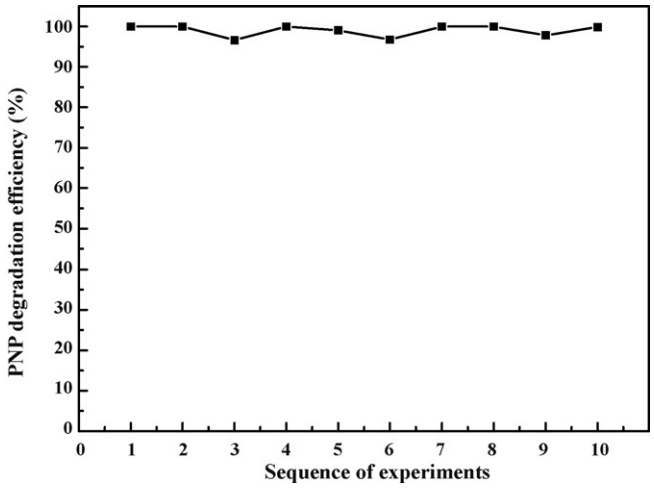

Fig. 9. PEC degradation efficiencies of PNP of 10 repeated experiments with SA-modified TiO_2 nanotube array electrode under UV light irradiation (1.0 mW/cm^2, 0.8 V vs SCE, 5 mg/L initial concentration of PNP, 0.01 M Na_2SO_4, 2 h irradiation time).

4. Conclusions

SA-modified TiO_2 nanotube array electrode has been fabricated and used in PEC degradation of PNP. This electrode absorbed well into the visible light region and exhibited a higher degradation efficiency of PNP compared with TiO_2 nanotube array electrode. The degradation efficiencies increased from 63 to 100% under UV light, and 79–100% under visible light ($\lambda > 400$ nm). The increase of the amounts of surface hydroxyl groups caused by the modification of SA, which accepted holes generated by solar or UV illumination to form hydroxyl radicals preventing electron–hole, was the main reason for the higher degradation efficiencies. According to the high degradation efficiency exhibited in this paper, the modification with the compounds containing hydroxyl groups on TiO_2 nanotube arrays might be used to improve the PC activity of TiO_2.

Acknowledgements

This work was supported by the National Nature Science Foundation of China (No. 20407005), and Hi-Tech Research and Development Program of China (No. 2007AA06Z406).

References

[1] M. Adachi, Y. Murata, J. Takao, J.T. Jiu, M. Sakamoto, F.M. Wang, Highly efficient dye-sensitized solar cells with a titania thin-film electrode composed of a network structure of single-crystal-like TiO_2 nanowires made by the "oriented attachment" mechanism, J. Am. Chem. Soc. 126 (2004) 14943–14949.
[2] X. Quan, N. Lu, J.Y. Li, S. Chen, H.T. Yu, G.H. Chen, Fabrication of boron-doped TiO_2 nanotube array electrode and investigation of its photoelectrochemical capability, J. Phys. Chem. C 111 (2007) 11836–11842.
[3] R. Molinari, R. Amadelli, A. Maldotti, P. Battioni, D. Mansuy, Phororedox and photocatalytic processes on Fe(III)-porphyrin surface modified nanocrystalline TiO_2, J. Mol. Catal. A 158 (2000) 521–531.
[4] W.K. Ho, J.C. Yu, J. Lin, J.G. Yu, P.S. Li, Preparation and photocatalytic behavior of MoS_2 and WS_2 nanocluster sensitized TiO_2, Langmuir 20 (2004) 5865–5869.
[5] S.U.M. Khan, M.A. Shahry, W.B. Ingler, Efficient photochemical water splitting by a chemically modified n-TiO_2, Science 297 (2002) 2243–2245.
[6] R. Asahi, T. Morikawa, T. Ohwaki, K. Aoki, Y. Taga, Visible-light photocatalysis in nitrogen-doped titanium oxides, Science 293 (2001) 269–271.
[7] X. Jiang, T. Wang, Influence of preparation method on morphology and photocatalysis activity of nanostructured TiO_2, Environ. Sci. Technol. 41 (2007) 4441–4446.
[8] S.L. Suib, L. Cao, T.N. Obee, S.O. Hay, Heterogeneous photocatalytic oxidation of 1-butene on SnO_2 and TiO_2 films, J. Phys. Chem. B 103 (1999) 2912–2917.
[9] C.K. Xu, S.U.M. Khan, R. Killmeyer, M.L. Gray, Photocatalytic effect of carbon-modified *n*-TiO_2 nanoparticles under visible light illumination, Appl. Catal. B 64 (2006) 312–317.
[10] K. Nagaveni, G. Madras, G. Sivalingam, M.S. Hegde, Solar photocatalytic degradation of dyes: high activity of combustion synthesized nano TiO_2, Appl. Catal. B 48 (2004) 83–93.

[11] S.X. Li, F.Y. Zheng, W.L. Cai, A.Q. Han, Y.K. Xie, Surface modification of nanometer size TiO_2 with salicylic acid for photocatalytic degradation of 4-nitrophenol, J. Hazard. Mater. B 135 (2006) 431–436.
[12] R.J. Candal, W.A. Zeltner, M.A. Anderson, Effects of pH and applied potential on photocurrent and oxidation rate of saline solutions of formic acid in a photoelectrocatalytic reactor, Environ. Sci. Technol. 34 (2000) 3443–3451.
[13] J.H. Park, S. Kim, A.J. Bard, Novel carbon-doped TiO_2 nanotube arrays with high aspect ratios for efficient solar water splitting, Nano Lett. 6 (2006) 24–28.
[14] W.T. Sun, Y. Yu, H.Y. Pan, X.F. Gao, Q. Chen, L.M. Peng, CdS quantum dots sensitized TiO_2 nanotube-array photoelectrodes, J. Am. Chem. Soc. 130 (2008) 1124–1125.
[15] A.D. Paola, V. Augugliaro, L. Palmisano, G. Pantaleo, E. Savinov, Heterogeneous photocatalytic degradation of nitrophenols, J. Photochem. Photobiol. A 155 (2003) 207–214.
[16] S. Sakthivel, M. Janczarek, H. Kisch, Visible light activity and photoelectrochemical properties of nitrogen-doped TiO_2, J. Phys. Chem. B 108 (2004) 19384–19387.